Topological Phase Transition in the Non-Hermitian Coupled Resonator Array

Yutian Ao,[1] Xiaoyong Hu,[1,2,3,*] Yilong You,[1] Cuicui Lu,[4,†] Yulan Fu,[5] Xingyuan Wang,[6,‡] and Qihuang Gong[1,2,3]

[1]*State Key Laboratory for Mesoscopic Physics & Department of Physics, Collaborative Innovation Center of Quantum Matter & Frontiers Science Center for Nano-optoelectronics, Beijing Academy of Quantum Information Sciences, Peking University, Beijing 100871, China*

[2]*Peking University Yangtze Delta Institute of Optoelectronics, Nantong, Jiangsu 226010, China*

[3]*Collaborative Innovation Center of Extreme Optics, Shanxi University, Taiyuan, Shanxi 030006, China*

[4]*Beijing Key Laboratory of Nanophotonics and Ultrafine Optoelectronic Systems, School of Physics, Beijing Institute of Technology, Beijing 100081, China*

[5]*Institute of Information Photonics Technology and School of Physics and Optoelectronics, Faculty of Science, Beijing University of Technology, Beijing 100124, China*

[6]*College of Mathematics and Physics, Beijing University of Chemical Technology, Beijing 100029, China*

(Received 17 December 2019; accepted 17 June 2020; published 1 July 2020)

In a two-dimensional non-Hermitian topological photonic system, the physics of topological states is complicated, which brings great challenges for clarifying the topological phase transitions and achieving precise active control. Here, we prove the topological phase transition exists in a two-dimensional parity-time-symmetric coupled-resonator optical waveguide system. We reveal the inherent condition of the appearance of topological phase transition, which is described by the analytical algebraic relation of coupling strength and the quantity of gain-loss. In this framework, the system can be switched between the topological and trivial states by pumping the site rings. This work provides a new degree of freedom to control topological states and offers a scheme for studying non-Hermitian topological photonics.

DOI: 10.1103/PhysRevLett.125.013902

Topological photonics provides a new platform to study the light-matter interactions and optical devices [1–3]. For example, robust topological edge states with their in-sight physics have great potential applications in lasers [4–6], quantum light sources [7], and reconfigurable pathways [8,9]. Though there has been great interest in topological photonics, the exploration of topological photonics has mainly been confined to the Hermitian regime. However, real systems are usually non-Hermitian. Advances in controlling gain and loss have provided mature methods in engineering non-Hermitian processes in photonic systems. Thus, studying non-Hermitian properties in topological photonics has the potential not only to utilize intrinsic loss, but also to achieve the purpose of realizing the active control of topological phase transition. Nevertheless, the investigation of non-Hermitian topological properties is difficult, resulting from the complexity of topological invariants [10]. What is worse, the principles of topological phase transition in Hermitian systems are not certain to still be valid in a non-Hermitian system.

Till now, studies of the non-Hermitian topological edge states were mainly constrained in one-dimensional systems, such as the plasmonic array [11,12], the parity-time (PT)-symmetric Su-Schrieffer-Heeger model [13–16], and the special constructed gain-loss chain [17]. Recently, a two-dimensional (2D) system with reconfigurable topological edge states controlled by pump light has been realized [18], showing the enormous potential for application of non-Hermitian photonics. However, clarifying the condition for the existence of topological phase transitions and achieving precise active control remains a great challenge in 2D non-Hermitian topological photonic systems.

Here, we prove that the topological phase transition exists in a 2D PT-symmetric coupled-resonator optical wave-guide (CROW) system. We reveal the inherent condition for the appearance of topological states, and we derive the analytical algebraic relation of coupling strength and the quantity of gain-loss describing the occurrence of the topological phase transition. What is more, the result can be generalized to arbitrary gain-loss configuration through a coordinate translation of gain and loss. Further discussions with a specific construction are carried out, showing the phase transition process with the field distribution and the transmission response.

The Hermitian CROW system is constructed of a site and link rings array, in which each site ring couples with four link rings, and each link ring couples with two site rings [19–22]. Site rings can be seen as the square lattice unit points, and link rings play the roles of their interactions. In order to demonstrate the existence of the topological states in the 2D non-Hermitian system and present the key role of the PT symmetry for the appearance of the topological states, we introduce the refractive-index modulation [23,24] with an even (odd) function for the real (imaginary)

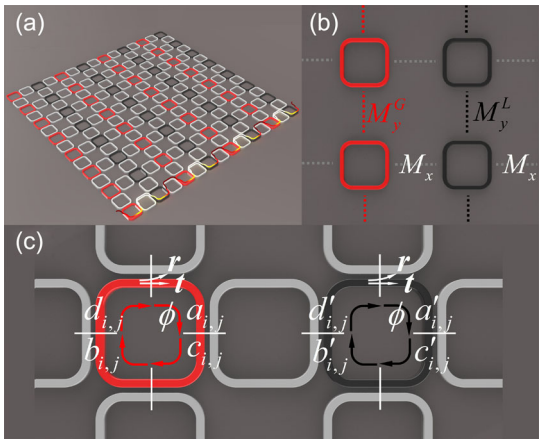

FIG. 1. (a) CROW system with a parity-time-symmetric lattice. Horizontally neighboring site rings are gain (red) and loss (black), while all the link rings (gray) are passive. A schematic topological edge mode is shown on the lower edge. (b) Coupling model of site rings. All link rings are replaced with dashed lines, and their couplings with site rings are abstracted into the transfer matrices, which are labeled on the model. (c) Unit cell of the lattice with field amplitudes, phase delay, and coupling coefficients labeled on it.

part of the refractive index in the array [Fig. 1(a)]. In the unit cell of our construction [Fig. 1(c)], the two neighboring site rings are set as gain (red) and loss (black) with equal quantities, while the link rings remain passive (gray). Note that the sizes of all rings are identical, meaning that the total optical path and the resonant frequency are the same among all rings.

We utilize the transfer matrix method to investigate the band structure of the system. The field amplitudes at the coupling position and the phase delay $\phi = \omega L_{\text{eff}}/4c$ (L_{eff} is the optical path of each ring) across one quarter of the ring are marked in Fig. 1(c). The propagation modes in site rings are set clockwise in our calculation. We define t and r as the transmission and coupling coefficients between site and link rings, respectively, as shown in Fig. 1(c). According to waveguide mode coupling theory, t is a real number, r is an imaginary number, and $|t|^2 + |r|^2 = 1$ is always satisfied. All the relations of field amplitudes between two neighboring site rings can be described by eight equations. For example, we set $d'_{i,j} = Ra_{i,j} + Tb'_{i,j}$, where

$$R = \frac{-rr^* e^{i2\phi}}{1 - t^2 e^{i4\phi}}, \qquad T = \frac{t(1 - e^{i4\phi})}{1 - t^2 e^{i4\phi}}. \tag{1}$$

Because of the space inversion symmetry, $c_{i,j} = Rb'_{i,j} + Ta_{i,j}$ is also tenable. As the CROW system is a periodic array, Floquet-Bloch theory is applied to get the relation between neighbor unit cells to describe the infinite array [25,26], which is $E_{i+1,j} = E_{i,j}e^{iK_x}$, $E_{i,j+1} = E_{i,j}e^{iK_y}$, where $E_{i,j}$ is the general term of the electric field amplitude of site rings. All the transfer matrices, which are shown in Fig. 1(b), can be expressed by the coupling parameters R and T, phase delay ϕ, Bloch phase K_x and K_y, and the quantity of gain (loss) κ. By building the simultaneous equations of all the coupling relations, we obtain the eigenvalue equation

$$e^{iK_x}\begin{pmatrix} b' \\ d' \end{pmatrix} = M_x M_y^G M_x M_y^L \begin{pmatrix} b' \\ d' \end{pmatrix}, \quad \text{where}$$
$$M_x = \frac{1}{R}\begin{pmatrix} 1 & -T \\ T & R^2 - T^2 \end{pmatrix},$$
$$M_y^G = \frac{1}{T}\begin{pmatrix} e^{-i2\phi}e^{-2\kappa} & -Re^{-iK_y} \\ Re^{iK_y} & (T^2 - R^2)e^{i2\phi}e^{2\kappa} \end{pmatrix},$$
$$M_y^L = \frac{1}{T}\begin{pmatrix} e^{-i2\phi}e^{2\kappa} & -Re^{-iK_y} \\ Re^{iK_y} & (T^2 - R^2)e^{i2\phi}e^{-2\kappa} \end{pmatrix}. \tag{2}$$

Here κ means that the field amplitudes increase (decrease) e^{κ} ($e^{-\kappa}$) times after traveling along a quarter of the whole ring. The band structure now can be derived based on Eq. (2). In the non-Hermitian case, the phase delay ϕ is $(\omega + i\omega_i)T_0$, where T_0 is the propagation time equal to $L_{\text{eff}}/4c$. Since frequency is a complex number, the band structure is described in the complex space as well. The imaginary bands characterize the corresponding mode gain or loss of the system [27]. Figure 2(a) shows the bulk band structures with four different κ's and a fixed coupling strength $t = 0.2$. As the frequency response of resonators is periodical, the band structure also has a period of normalized $\Delta\omega = 1$. It can be found that the band structure of the PT symmetry system shows band inversion, which is the typical characteristic of the topological phase transition [28–30]. With the increase of κ, the two bands in one period get closer and form a Dirac point. Then the Dirac point opens up a new band gap when κ further gets larger. The corresponding projected band is also investigated with 50 unit cells along the y direction of the array to provide the information of edge states. It can be seen that edge states between the two bulk bands disappear in the new gap after the Dirac point opens up. This band inversion is exactly the topological phase transition, which is similar in the Hermitian CROW system.

In the band structure calculation, we find that Dirac points always appear at

$$\omega = \left(N - \frac{1}{2}\right)\frac{2\pi c}{L_{\text{eff}}}, \tag{3}$$

where N denotes the periodicity of frequency. Therefore, the phase delay can be derived as

$$\phi = \frac{\pi}{4} + N\frac{\pi}{2}, \tag{4}$$

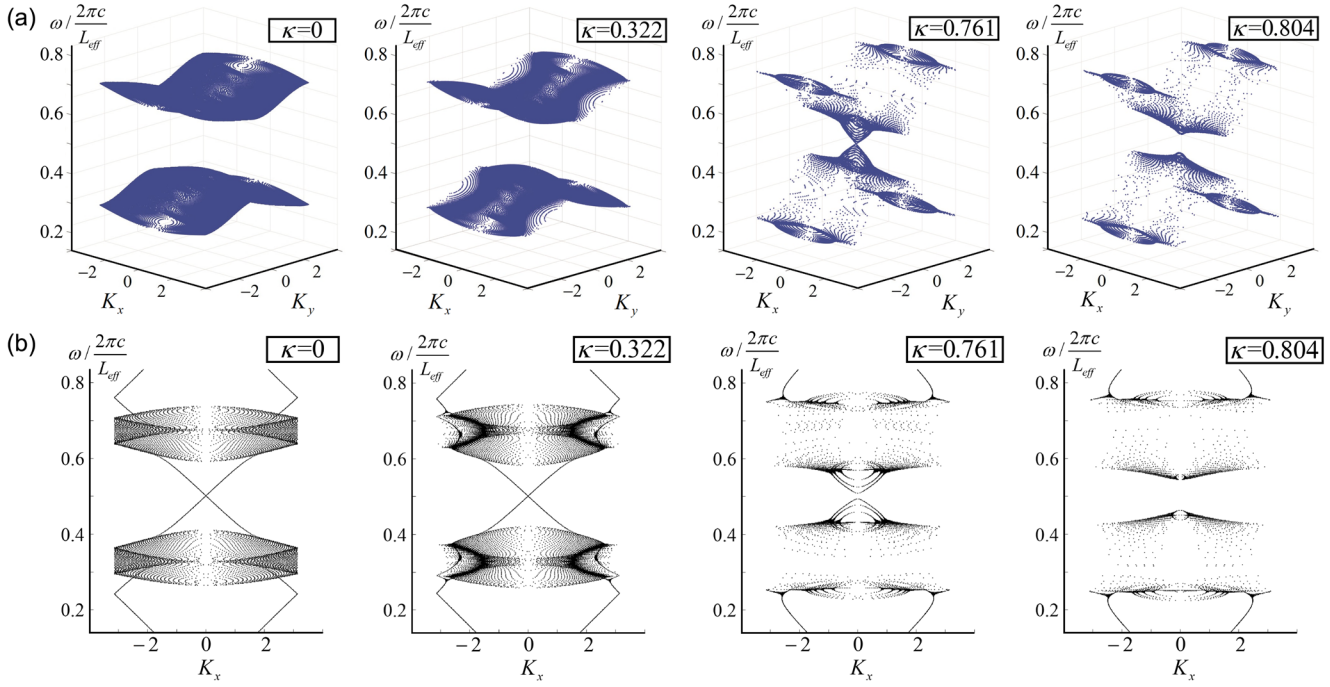

FIG. 2. (a) and (b): Bulk and projected band structures of the real frequency with different gain-loss quantities κ and a fixed coupling strength $t = 0.2$, respectively. When $\kappa < 0.761$, there are topological edge states in the band gap. Two bulk bands get closer to form a Dirac point until $\kappa = 0.761$. The Dirac point opens up a new gap without any edge state in it when $\kappa > 0.761$.

indicating the frequency corresponds to the destructive interference of each ring. Dirac points are located at the Γ point ($K_x = K_y = 0$) in the Brillouin zone. Thus, at Dirac points, Eq. (1) is simplified as

$$R = i\sin\gamma, \qquad T = \cos\gamma, \tag{5}$$

where $\gamma = \arctan(1 - t^2/2t)$ is a reduced coupling parameter. The transfer matrix is then written as

$$M_x = \frac{1}{i\sin\gamma}\begin{pmatrix} 1 & -\cos\gamma \\ \cos\gamma & -1 \end{pmatrix},$$
$$M_y^G = \frac{i}{\cos\gamma}\begin{pmatrix} e^{-2\kappa} & -\sin\gamma \\ \sin\gamma & -e^{2\kappa} \end{pmatrix},$$
$$M_y^L = \frac{i}{\cos\gamma}\begin{pmatrix} e^{2\kappa} & -\sin\gamma \\ \sin\gamma & -e^{-2\kappa} \end{pmatrix}. \tag{6}$$

The condition for Dirac points to exist is that the eigenvalue equation have a solution, and it requires

$$|M_x M_y^G M_x M_y^L - I| = 0. \tag{7}$$

Through solving this equation, a simple relation is obtained as

$$\tan\gamma = \cosh 2\kappa. \tag{8}$$

This relation describes a topological phase boundary in the phase diagram shown in Fig. 3. The phase diagram indicates that the topological edge state can appear in the non-Hermitian system with PT symmetry. In previous Hermitian systems, the topological phase transition could only be realized by tuning the coupling strengths of the system—i.e., the topological phase transition only occurred along the horizontal blue line shown in Fig. 3. In this non-Hermitian system, the topological phase transition can also appear along the vertical green line with the variation of κ. In order to investigate the topological phase transition in this new degree of freedom, we calculate the band structures for $\kappa = 0$, $\kappa = 0.322$, $\kappa = 0.761$, and $\kappa = 0.804$ with a fixed coupling strength $\gamma = \arctan 2.4$ (Fig. 2). The first two points are located at the topological nontrivial region, for which the topological edge states appear in the band gap in Fig. 2(b). The third value is exactly on the phase boundary, which corresponds to the case that the band forms a Dirac point. The last point is located in the trivial region, and edge states disappear in the band gap.

A generalized derivation with the arbitrary gain and loss of two site rings in the unit cell is investigated in the Supplemental Material [27]. Quantities κ_1 and κ_2 replace κ and $-\kappa$ in the transfer matrices [Eq. (6)], and the result is that only when the quantity of gain and loss is equal (i.e., $\kappa_1 + \kappa_2 = 0$) does Eq. (7) have a solution, which means the PT configuration is a key condition in this framework to support such a topological phase transition. However, this derivation has a basic assumption—that the eigenvalue of the Dirac point is a real number. In fact, it can also be a

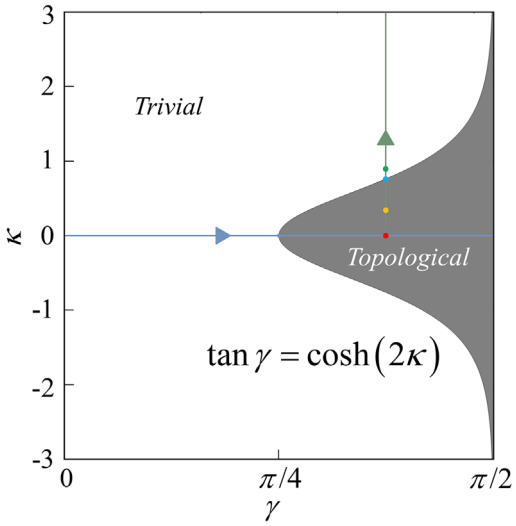

FIG. 3. Topological phase diagram of coupling strength γ and gain-loss quantity κ. The relation $\tan\gamma = \cosh 2\kappa$ is plotted on the diagram, which is the boundary of topological phase transition. The blue line denotes the topological phase transition process in the Hermitian system with the variation of γ. The green line denotes the topological phase transition process under the variation of κ with a fixed γ ($\tan\gamma = 2.4$), on which four dots with different colors are highlighted, exactly corresponding to the four quantities of gain-loss in Fig. 2.

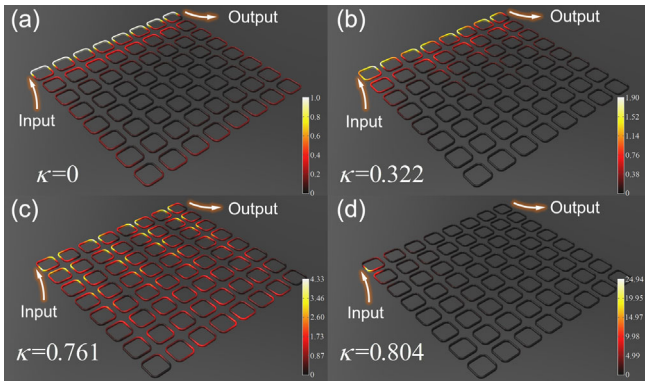

FIG. 4. The electric field distribution under different gain-loss quantities κ. An 8×8 CROW array is solved numerically based on the transfer matrix method with accurate coupling conditions. The input is set on the upper-left corner, and the output is set on the upper-right corner. The frequency of input light is selected close to the Dirac point—that is, $\omega = 0.46$. The parameters κ of each diagram correspond to the dots in Fig. 3.

complex number, which means the eigenstate has gain or loss. When $\kappa_1 \neq -\kappa_2$, the edge states can still exist, but the modes corresponding to the edge states have a nonzero imaginary part. When the system loss is greater (less) than the gain, the edge states propagate with a loss (gain) transmission. Therefore, such topological phase transition only depends on the contrast of κ_1 and κ_2 (even when they are both positive). The edge states will maintain and be enhanced (attenuated) with the increase (decrease) of κ_1 or κ_2 when the contrast $\kappa_1 - \kappa_2$ is small to stay in the topological region; but when the contrast of $\kappa_1 - \kappa_2$ is large enough to go into the trivial region, the transmission of edge states will start to decline and finally lead to the forbidden state with the increase (decrease) of κ_1 or κ_2. In addition, since arbitrary gain and loss are equivalent to a PT-symmetric configuration with a uniform background of gain or loss, the behavior of edge modes can also be obtained based on the PT-symmetric case with a background gain or loss.

The electric field distribution of a PT-symmetric CROW array with 8×8 site rings is numerically obtained using the transfer matrix method. The input and output channels are set, completely coupling with the site rings on the upper-left and upper-right corners, respectively. The coupling strength in the array still meets $\tan\gamma = 2.4$, corresponding to the vertical green line in Fig. 3, and the normalized frequency ω in the numerical calculation is selected at 0.46, close to the Dirac point frequency. Figure 4 shows the electric field distribution of a CROW array with the same four quantities of gain and loss as those of the band structures. Because we are mainly concerned about the field in site rings, we leave out link rings in the figure. Figure 4(a) shows the ordinary topological edge state, which is the Hermitian case as $\kappa = 0$. In Fig. 4(b), $\kappa = 0.322$, the system is in the topological region. The edge state still exists, but the energy gets gain (loss) in gain (loss) rings. Note that the gain and loss just counteract each other, well matching with the zero mode gain or loss of the edge states reflected by the imaginary part of the band structure [27]. In Fig. 4(c), the field distribution shows a bulk state with $\kappa = 0.761$, which is consistent with band structure. Finally, the system evolves into the trivial region as κ increases to 0.804. Light cannot travel into the array, and nearly all the energy travels back to the input channel [Fig. 4(d)].

Further, we analyze the transmission properties with the variation of κ under different γ values to quantitatively discuss the effect of controlling the topological phase transition in an array with 5×5 unit cells. Figure 5(a) presents the transmission spectra with four coupling strengths γ in the topological nontrivial region and four γ in the trivial region. The four spectra corresponding to larger coupling strengths exhibit transition points which are responses of the topological phase transitions, while the other four decrease smoothly. For the four larger γ values, the topological phase transition happens when κ increases to the value decided by Eq. (8). The transmission sharply decreases as the system evolves into the trivial region. The dashed lines are the exact phase transition positions solved by Eq. (8). The mismatching between the transition points and the accurate position is resulting from the finite array [27], and it will be smaller when the calculated array gets larger.

Finally, we illustrate the topological phase transition in the view of band inversion. The eigenmodes at the top of the lower band and bottom of the upper band are calculated

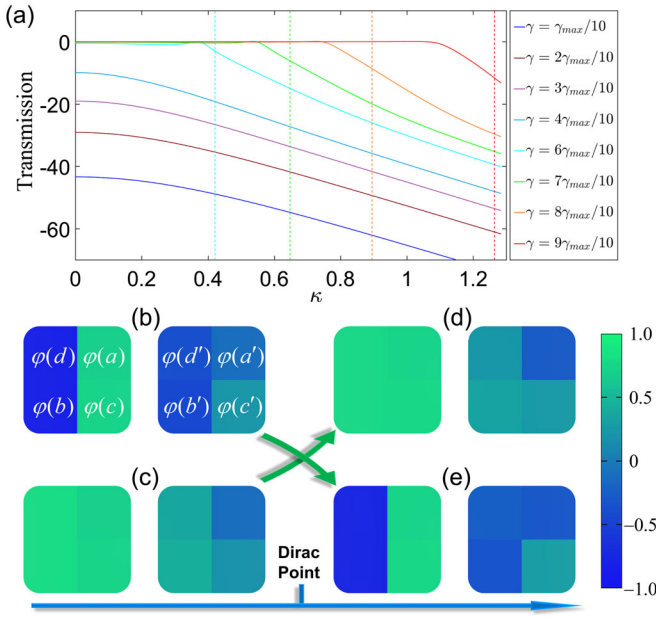

FIG. 5. (a) The transmission varies with gain-loss quantity κ under different coupling strengths γ, where $\gamma_{\max} = \pi/2$. The model has the same configuration as Fig. 4, but with only five unit cells. (b)–(e): The eigenmodes of two neighboring bulk bands at Γ points before and after the topological phase transition. The modes of upper (b) and lower (c) bands reverse to those of lower (e) and upper (d) bands across the phase transition, respectively. The band inversion happens associated with the topological phase transition.

before and after the phase transition point. As the module values of eigenmodes at the two bands are the same, the phases of field amplitudes are key elements to describe their differences. $\varphi(E)$ is defined as $real(E)/|E|$ to form the eigenmode diagrams shown in Figs. 5(b)–5(e). The four diagrams are the modes at the upper band [Figs. 5(b) and 5(d)] and the lower band [Figs. 5(c) and 5(e)] before and after the phase transition point, respectively. Figure 5 clearly shows that the eigenmodes exchange their positions with each other in the process of the phase transition, indicating the bands are inverted.

In conclusion, we demonstrate the existence of the topological phase transition in a PT-symmetric CROW system. An analytical algebraic relation $\tan\gamma = \cosh 2\kappa$ is derived, revealing the precise condition of the appearance of the topological phase transition decided by coupling strength γ and quantity of gain-loss κ in the PT-symmetric system. It is found that such phase transition only depends on the gain-loss contrast, especially for the PT-symmetric configuration, providing neutral topological edge states. The topological phase transition process is clearly verified by the field distribution, the transmission response, and the band inversion. This research provides a new degree of freedom to modulate the topological phase transition and guide the realization of the active control of the topological states. Besides this, the work presents the condition for exploring topological phase transitions in high-dimensional non-Hermitian systems.

We are grateful for helpful discussions from Professor C. T. Chan's group at the Hong Kong University of Science and Technology, and Professor Yong-Chun Liu at Tsinghua University during the review process. This work was supported by the National Key Research and Development Program of China under Grants No. 2018YFB2200403 and No. 2018YFA0704404; by the National Natural Science Foundation of China under Grants No. 61775003, No. 11734001, No. 91950204, No. 11527901, No. 91850117, No. 11704017, No. 11734001, and No. 11654003; by Beijing Municipal Science & Technology Commission No. Z191100007219001; by Beijing Natural Science Foundation No. Z180015; and by the Beijing Institute of Technology Research Fund Program for Young Scholars.

*Corresponding author.
xiaoyonghu@pku.edu.cn
†Corresponding author.
cuicuilu@bit.edu.cn
‡Corresponding author.
wang_xingyuan@mail.buct.edu.cn

[1] F. D. M. Haldane and S. Raghu, Phys. Rev. Lett. **100**, 013904 (2008).
[2] L. Lu, J. D. Joannopoulos, and M. Soljačić, Nat. Photonics **8**, 821 (2014).
[3] T. Ozawa, H. M. Price, A. Amo, N. Goldman, M. Hafezi, L. Lu, M. C. Rechtsman, D. Schuster, J. Simon, O. Zilberberg *et al.*, Rev. Mod. Phys. **91**, 015006 (2019).
[4] G. Harari, M. A. Bandres, Y. Lumer, M. C. Rechtsman, Y. D. Chong, M. Khajavikhan, D. N. Christodoulides, and M. Segev, Science **359**, eaar4003 (2018).
[5] M. A. Bandres, S. Wittek, G. Harari, M. Parto, J. Ren, M. Segev, D. N. Christodoulides, and M. Khajavikhan, Science **359**, eaar4005 (2018).
[6] S. Longhi, Y. Kominis, and V. Kovanis, Europhys. Lett. **122**, 14004 (2018).
[7] S. Mittal, E. A. Goldschmidt, and M. Hafezi, Nature (London) **561**, 502 (2018).
[8] X. Cheng, C. Jouvaud, X. Ni, S. H. Mousavi, A. Z. Genack, and A. B. Khanikaev, Nat. Mater. **15**, 542 (2016).
[9] D. Leykam, S. Mittal, M. Hafezi, and Y. D. Chong, Phys. Rev. Lett. **121**, 023901 (2018).
[10] D. Leykam, K. Y. Bliokh, C. Huang, Y. D. Chong, and F. Nori, Phys. Rev. Lett. **118**, 040401 (2017).
[11] S. R. Pocock, P. A. Huidobro, and V. Giannini, Nanophotonics **8**, 1337 (2019).
[12] S. Ke, B. Wang, H. Long, K. Wang, and P. Lu, Opt. Express **25**, 11132 (2017).
[13] Z. Turker, S. Tombuloglu, and C. Yuce, Phys. Lett. A **382**, 2013 (2018).
[14] B. Wu, J. Wang, M. Xiao, J. Xu, and Y. Chen, Opt. Express **25**, 1040 (2017).

[15] H. Zhao, P. Miao, M. H. Teimourpour, S. Malzard, R. El-Ganainy, H. Schomerus, and L. Feng, Nat. Commun. **9**, 981 (2018).
[16] M. Pan, H. Zhao, P. Miao, S. Longhi, and L. Feng, Nat. Commun. **9**, 1308 (2018).
[17] K. Takata and M. Notomi, Phys. Rev. Lett. **121**, 213902 (2018).
[18] H. Zhao, X. Qiao, T. Wu, B. Midya, S. Longhi, and L. Feng, Science **365**, 1163 (2019).
[19] G. Q. Liang and Y. D. Chong, Phys. Rev. Lett. **110**, 203904 (2013).
[20] F. Gao, Z. Gao, X. Shi, Z. Yang, X. Lin, H. Xu, J. D. Joannopoulos, M. Soljačić, H. Chen, L. Lu *et al.*, Nat. Commun. **7**, 11619 (2016).
[21] M. Hafezi, E. A. Demler, M. D. Lukin, and J. M. Taylor, Nat. Phys. **7**, 907 (2011).
[22] M. Hafezi, S. Mittal, J. Fan, A. Migdall, and J. Taylor, Nat. Photonics **7**, 1001 (2013).
[23] A. Cerjan, A. Raman, and S. Fan, Phys. Rev. Lett. **116**, 203902 (2016).
[24] A. Mock, Phys. Rev. A **95**, 043803 (2017).
[25] A. Yariv, Y. Xu, R. K. Lee, and A. Scherer, Opt. Lett. **24**, 711 (1999).
[26] J. K. Poon, J. Scheuer, S. Mookherjea, G. T. Paloczi, Y. Huang, and A. Yariv, Opt. Express **12**, 90 (2004).
[27] See Supplemental Material at http://link.aps.org/supplemental/10.1103/PhysRevLett.125.013902 for the imaginary part of the band structure, derivation with arbitrary gain and loss, and other supplementary discussions.
[28] Z.-G. Chen and Y. Wu, Phys. Rev. Applied **5**, 054021 (2016).
[29] L. Xu, H.-X. Wang, Y.-D. Xu, H.-Y. Chen, and J.-H. Jiang, Opt. Express **24**, 18059 (2016).
[30] Y. Yang, Y. F. Xu, T. Xu, H.-X. Wang, J.-H. Jiang, X. Hu, and Z. H. Hang, Phys. Rev. Lett. **120**, 217401 (2018).